Enhanced cooling system with integrated multi-geothermal concept– numerical and experimental studies

Rabih Murr, Jalal Faraj, Elias Harika, Cathy Castelain, Mahmoud Khaled

Enhanced cooling system with integrated multi-geothermal concept– Numerical and experimental studies

Rabih Murr[1], Jalal Faraj[2,3], Elias Harika[1], Cathy Castelain[4], and Mahmoud Khaled[2,5,*]

[1]*Energy and Thermo-Fluid group – Lebanese International University LIU – Bekaa – Lebanon*
[2]*Energy and Thermo-Fluid group – International University of Beirut BIU – Beirut – Lebanon*
[3]*Lebanese University, Faculty of Technology, Saida, Lebanon*
[4]*Laboratory of Thermal Energy of Nantes, LTEN, Polytech' Nantes, University of Nantes, Nantes-France*
[5]*University Paris Diderot, Sorbonne Paris Cité, Interdisciplinary Energy Research Institute (PIERI), Paris, France*
**Corresponding author: mahmoud.khaled@liu.edu.lb*

Abstract: In order to reduce the energy bills and pollution of buildings due to the use of conventional cooling systems, the present paper presents a parametric analysis and a case study concerning a newly proposed Multi Geothermal Cooling System that uses the cold soil to precool or cool air of several residences simultaneously. For that purpose, a thermal modelling and a related in-house code are developed. The modelling allows to predict the temperature of the precooled (or cooled) air in function of the return air temperature (hot flow) and the mass flow rate. The effect of other governing parameters has been evaluated, like the depth in soil, the tubes length and diameter. Modelling results have been confronted to experimentation showing a worst case error of 1.9°C in the precooled air temperature. The work doesn't stop here. The predicted air temperature has been used in a numerical study of a multi geothermal cooling system with air-conditioning systems and different scenarios were simulated. Energy savings and reduction in CO_2 emission have been evaluated for different coefficients of performance. Results are promising and relevant recommendations were put on firm roots.

Keywords: Multi Geothermal Cooling System, Buried Pipes, Thermal Modelling, Parametric Analysis, In-house Code, Case Study.

1- Introduction

It is well known that summer is a time for warm temperatures. Personal comfort and health are strongly affected by the high temperature and the humidity or the moisture content of the air. In countries known to have hot summers, refrigeration cooling systems or air conditioning systems are frequently used for improving the indoor environments of buildings and making lives healthier and much more productive. The running cost of air condition systems is often the most significant of the buildings bills. These systems, that use an electric compressor and electric fans, consume a non-negligible electric power.

In order to minimize the electric energy "E" consumed by the air conditioning systems to a value "α.E' where "α" is a fraction between 0 and 1 and then to reduce their running cost and their contribution to the environment pollution, alternative solutions should be adopted. One of them is to use sustainable building materials [1-2] or a cheaper source of electric energy like renewable energy [3-7] sources: solar energy [8-12], wind energy [13-18] and geothermal energy [19-25]. The other solution is to reduce the cooling power that the air conditioning systems should ensure by reducing the temperature of the air by cooling or pre-cooling the air supplied to or within a building by a free source like geothermal energy [26-38] when the temperature of the ground soil is lower than the ambient temperature. In this case, air will flow through

buried pipes that are used as earth-to-air heat exchangers where air releases its energy to soil since its temperature is almost constant at a certain depth throughout the year, which allows using it as a heat sink in summer.

Several studies have been conducted on buried pipes worldwide. Krarti and Kreider [39] developed a simplified model that permits to determine the energy performance of an underground air tunnel. They conducted a parametric study to determine the impact of the hydraulic diameter of the tunnel and the flow rate of the air on the heat transfer between the air and ground. This model has been validated experimentally. Al Ajmi et al. [40] developed a theoretical model of an earth–to-air heat exchanger that permits to calculate the outlet air temperature and the cooling potential of such device in hot climates. Simulation results showed that this heat exchanger allows reducing the cooling energy by 30% during the hotter summer season.

Kumar et al. [41] proposed a computer design tool that permits to evaluate any aspect of earth-to-air heat exchanger based on the concept of artificial neural network. This developed tool is suitable for the calculation of the outlet air temperature and the cooling potential of the earth-to-air heat exchanger system. The results showed that the thermal performance of these heat exchangers is influenced by several variables like: ambient air temperature, heat exchanger length, ground temperature, humidity, air mass flow rate and ground surface temperature. Amit et al. [42] tested an underground room heating and cooling system. Four types of buried pipes of different materials (PVC, MS, PVC filtered and Bamboo) were installed to study the heat transfer between ambient air passing through the pipes and the soil. All these pipes have a length of 30 feet and are dug 8 feet deep and an air flow at 4.5 m/s was provided. A change in air temperature was found but the cooling and heating rates depends on the temperature of the inlet air and the pipes material. A considerable amount of heating power was obtained from PVC, MS and PVC filtered pipe. Bamboo provided a reduced heating performance. On the other hand, a considerable amount of cooling power was obtained with bamboo while the other pipes had less cooling properties. Mihalakakou et al. [43] examined the heating potential of a single earth- to- air heat exchanger and a multiple parallel earth tubes system. They developed an accurate numerical model to investigate the dynamic thermal performance of these systems during the winter period in Dublin. The results showed that the heating potential is essential. They also studied the impact of the tubes length, tubes diameter, air velocity inside the tubes and the depth in soil. The obtained results showed that the effectiveness of the earth-to-air heat exchanger increases when the tubes length increases (checked range 30 m to 70 m) and when the depth in soil increases. But, it decreases when the tubes diameter increases from 0.1 m to 0.15 m because the convective heat transfer coefficient between the air and the inner surface of the tubes decreases and when the air velocity increases (checked range 5 m/s to 15 m/s) because the mass flow rate will increase. Manoj et al. [44] perform experiments on an earth-to-air heat exchanger system in the summer climate. Experimental results showed that the drop in air temperature between the inlet and outlet of the pipe decreases from 8.6 to 4.18 °C when the air velocity increases from 4.1 to 11.6 m/s.

Based on what is presented above, it can be concluded that the use of buried pipes in cooling or heating systems within the context of geothermal energy is one of the promising solutions nowadays to reduce the energy consumption and the CO_2 emissions. This research area deserves a special attention especially when it comes to have a complete numerical and experimental study that permits to study the effect of the main parameters of the heat exchanger on the performance of the system. However, scarce are the studies that combine together many systems of geothermal cooling systems using buried pipes to serve simultaneously many residences and increase the system performance and efficiency when needed. Furthermore, scarce are the studies that treat the impact of critical parameters on the system by using a simplified thermal model. For that purpose, the present paper proposes a new Multi Geothermal Cooling System (MGCS) that uses the relatively cold soil to cool/precool air of the cooling system of several residences simultaneously. A thermal modelling is validated experimentally and a parametric study is performed. Moreover, energetic and environmental studies have been done for the case of Lebanon.

The originality of the present paper is shown through the following points:

1. It proposes a new system that allows enhancing the performance of geothermal air cooling systems.
2. A parametric study can be performed easily with low computational time in addition to the thermal modelling of the geothermal air cooling system.
3. It offers useful system and model for geothermal systems.
4. This work also permits to assess the impact of different parameters on the performance of the system.

This paper is organized as follows. The concept of the Multi Geothermal Cooling System (MGCS) is presented in section 2. Section 3 presents the thermal modelling. The in-house code is presented in section 4. Section 5 presents the experimental procedure and the validation of the thermal model. A parametric study is shown in section 6. In section 7, energetic and environmental studies are presented for the case of Lebanon. Finally, section 8 underlines the main conclusions of the paper.

Nomenclature

α - fraction
PVC – Polyvinyl chloride
MS – mild steel
$\dot{Q}$ - rate of heat, W;
$\dot{m}_a$ - mass flow rate of air, kg/s;
Cp_a - the specific heat of air, kJ/kg.K
ΔT_a - air temperature difference, K;
V - speed, m/s;
A_c - cross sectional area, m^2;
ρ - density of air, kg/m^3;
d_i - inner diameter of the buried tubes, m;
ΔT_{ln} - logarithmic mean temperature difference, K;
R_{tot} - total thermal resistance, K/W;
$R_{conv\,(air,tube)}$ - convection resistance between the air and the inner surface of the tubes, k/W;
$R_{cond\,(tube)}$ - conduction resistance of the tubes, k/W;
$R_{cond\,(soil)}$ - conduction resistance of the soil, k/W;
h_{air} - convective heat transfer coefficient between the air flowing inside the tubes and the inner surface of the tubes, $W/m^2.K$;
$A_{L,i}$, - lateral area of the inner surface of the tubes, m^2;
L - length of the tubes, m;
Re - Reynolds number;
$\mu_{a,i}$ - dynamic viscosity of the air, Pa.s;
Nu - Nusselt number;
P_r - Prandtl number;
k_{air} - thermal conductivity of the air, W/m.K;
k_{tube} - thermal conductivity of the tube, W/m.K;
P – Pressure, Pa;
R – gas constant, J/kg.K ;
Z - depth in soil, m;
k_{soil} - soil thermal conductivity, W/m.K;
d_o - outer diameter of the tubes, m;
E - Energy reduced, kWh;
t – time, hours;
C - Cost, $;
M – mass, kg
β – Coefficient of performance.

Subscripts

a – air;
c – cross section;
i – inner;
tot – total;
$conv$ – convection;
$cond$ – conduction;
L – lateral.

2- Concept of the multi geothermal cooling system

Figure 1 shows the schematic of the Multi Geothermal Cooling System (MGCS) that uses the relatively cold soil to cool/precool air of the cooling system of several residences, rooms, and apartments simultaneously. The geothermal air cooling system consists of air tubes buried in soil at a given depth "z". Fresh ambient air, return indoor air (from the residence) or mixed air enters the buried tubes where it releases heat to the soil through the lateral area of the tubes. Then, colder air exits the geothermal air cooling system and enters the residence. A fan could be used to ensure the flowing of air within the tubes. The main advantage of using the return air from the space is that it is colder than the ambient air; so it can be cooled more.

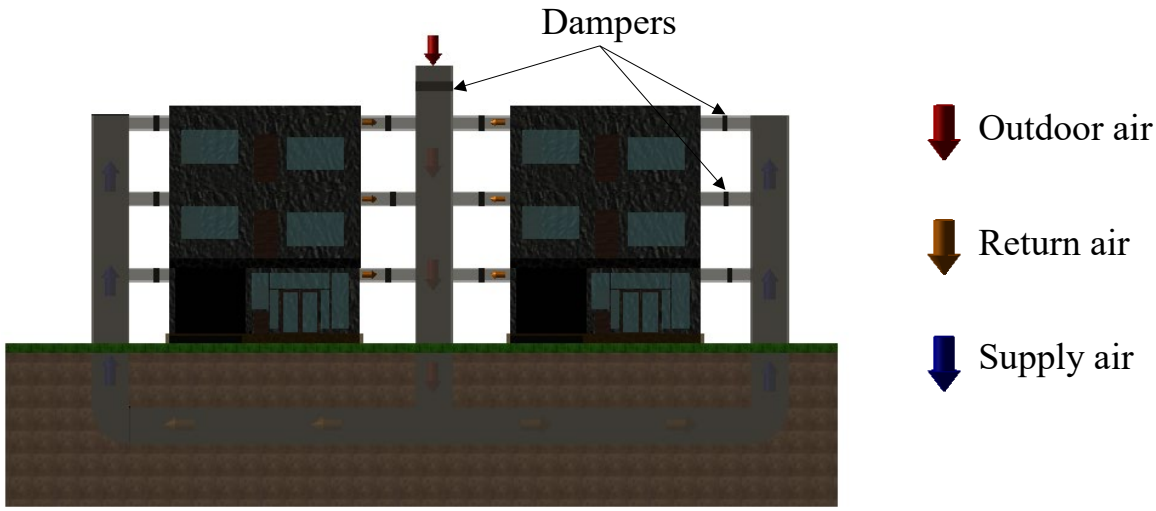

Fig. 1. Schematic of the multi geothermal cooling system.

As shown in Fig. 1, the opening and closing of the dampers control the flow rates of the outdoor fresh air, the return air from each apartment of each building and the supply air to each apartment of each building. The system presented in Fig. 1 is a first draft. Additional accessories like valves and connections will be presented in future works.

3- Thermal modelling

A thermal modelling of a geothermal air cooling system is developed and is detailed in this part. This model relies on the mass and energy conservation principles with steady state conditions.

The rate of heat loss by the air flowing through the tubes or the cooling power is calculated using the following equation:

$$\dot{Q} = \dot{m}_a \cdot Cp_a \cdot \Delta T_a \qquad (1)$$

Where:

- $\dot{m}_a$ is the mass flow rate of air, kg/s;
- Cp_a is the specific heat of air, kJ/kg.K;
- ΔT_a is the temperature difference of air between the inlet and the outlet ($T_{a,i} - T_{a,o}$) of the buried tubes, K.

The mass flow rate of air is calculated using the following equation:

$$\dot{m}_a = \rho \cdot A_c \cdot V \qquad (2)$$

Where:

- V is the air speed within the buried tubes, m/s;
- A_c is the cross sectional area of the tubes, m^2;
- ρ is the density of air, kg/m^3.

The density ρ of air is obtained from the ideal gas equation:

$$P = \rho \cdot R \cdot T_{a,i} \qquad (3)$$

Where:

- P is the atmospheric pressure, Pa;
- R is the gas constant for air, 287 J/kg.K;
- $T_{a,i}$ is the temperature of the air at the inlet conditions of the tubes, K.

The cross sectional area "A_c" is obtained from the following equation:

$$A_c = \frac{\pi \cdot d_i^2}{4} \qquad (4)$$

Where:

- d_i is the inner diameter of the buried tubes, m.

Also, the rate of heat transfer ($\dot{Q}$) can be calculated using the following equation:

$$\dot{Q} = \Delta T_{\ln} \Big/ R_{tot} \qquad (5)$$

Where:

- $\Delta T_{\ln}$ is the logarithmic mean temperature difference between the air temperatures ($T_{a,i}$ and $T_{a,o}$) and the soil temperature (T_{soil}), K;
- R_{tot} is the total thermal resistance between the air and the soil, K/W.

$\Delta T_{\ln}$ is given by the following equation:

$$\Delta T_{\ln} = \frac{((T_{a,i} - T_{soil}) - (T_{a,o} - T_{soil}))}{\ln((T_{a,i} - T_{soil})/(T_{a,o} - T_{soil}))} \quad (6)$$

The total thermal resistance R_{tot} is the sum of three thermal resistances in series and it can be calculated using the following equation:

$$R_{tot} = R_{conv\,(air,tube)} + R_{cond\,(tube)} + R_{cond\,(soil)} \quad (7)$$

Where:

- $R_{conv\,(air,tube)}$ is the convection thermal resistance between the air and the inner surface of the tubes, K/W;
- $R_{cond\,(tube)}$ is the conduction thermal resistance of the tubes, K/W;
- $R_{cond\,(soil)}$ is the conduction thermal resistance of the soil, K/W.

Fig. 2 shows the three thermal resistances between the soil temperature (T_{Soil}) and the air temperature inside the tubes (T_a).

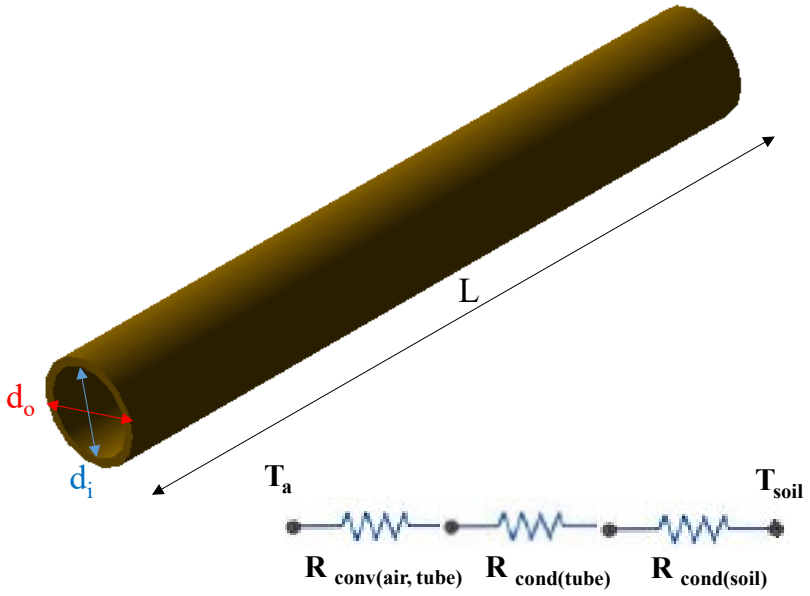

Fig. 2. The three thermal resistances between T_{Soil} and T_a

The convective thermal resistance between the air and the inner surface of the tubes $R_{conv\,(air,tube)}$ can be calculated as follows:

$$R_{conv\,(air,tube)} = \frac{1}{h_{air} \cdot A_{L,i}} \qquad (8)$$

Where:

- h_{air} is the convective heat transfer coefficient between the air flowing inside the tubes and the inner surface of the tubes, W/m^2.K;
- $A_{L,i}$ is the lateral area of the inner surface of the tubes, m^2. It is given as follows:

$$A_{L,i} = \pi \cdot d_i \cdot L \qquad (9)$$

Where:

- d_i is the inner diameter of the tubes, m;
- L is the length of the tubes, m.

The heat transfer coefficient "h_{air}" is calculated by using equations (10-12):

$$R_e = \frac{\rho \cdot V \cdot d_i}{\mu_a} \qquad (10)$$

$$Nu = 0.023 \times R_e^{0.8} \times P_r^{0.3} \text{ (if turbulent flow, Re} \geq 2300) \qquad (11\text{-a})$$

$$Nu = 3.66 \text{ (if laminar flow, Re} < 2300) \qquad (11\text{-b})$$

Where:

- R_e is the Reynolds number of the air;
- P_r is the Prandtl number of the air.
- μ_a is the dynamic viscosity of the air, Pa.s;
- Nu is the Nusselt number of the air;

$$h_{air} = \frac{Nu \cdot k_{air}}{d_i} \qquad (12)$$

Where:

- k_{air} is the air thermal conductivity, W/m.K.

All air properties are calculated at the average temperature of air between the inlet and outlet.

The conductive thermal resistance of the tube $R_{cond\,(tube)}$ is calculated as follows:

$$R_{cond(tube)} = \frac{\ln(d_o / d_i)}{2 \cdot \pi \cdot k_{tube} \cdot L} \quad (13)$$

Where:

- k_{tube} is the tube thermal conductivity, W/m.K.

The conductive thermal resistance of the soil $R_{cond(soil)}$ is calculated from the conductive factor (S) using equations (14) and (15):

$$R_{cond(soil)} = \frac{1}{S} \quad (14)$$

$$S = \frac{2 \cdot \pi \cdot L \cdot k_{soil}}{\ln(\frac{8 \cdot Z}{\pi \cdot d_o})} \quad (15)$$

Where:

- Z is the depth in soil, m;
- k_{soil} is the soil thermal conductivity, W/m.K;
- d_o is the outer diameter of the tubes, m.

4- In-house code

In order to simulate numerically the proposed geothermal air cooling system, an in-house code is developed. This code consists of a procedure of calculation that uses a set of input parameters and the equations presented in the thermal modelling to determine the main outputs: the supply air temperature ($T_{a,o}$), the air mass flow rate ($\dot{m}_a$) and the cooling power ($\dot{Q}$). The main input parameters that are considered are: the atmospheric pressure, the tubes inlet air temperature or the atmospheric air temperature, the properties of the tubes (inner diameter, outer diameter and conductivity), the properties of air (specific heat, thermal conductivity and dynamic viscosity), the tubes length (L), the soil temperature, the soil conductivity, the depth of the tubes and the air speed within the tubes. Fig. 3 shows a schematic of the inputs and outputs of the computational code.

The procedure of calculation begins with an initialization step that defines the inputs of the system. Then, a calculation step using the equations presented in the thermal modelling is performed to determine the other parameters. The iterative phase consists of determining the heat capacity of the buried tubes in two different ways and looping it until the difference between them is less or equal to a small ε equal to 0.1 %. Fig. 4 shows the algorithm with the detailed steps of the code.

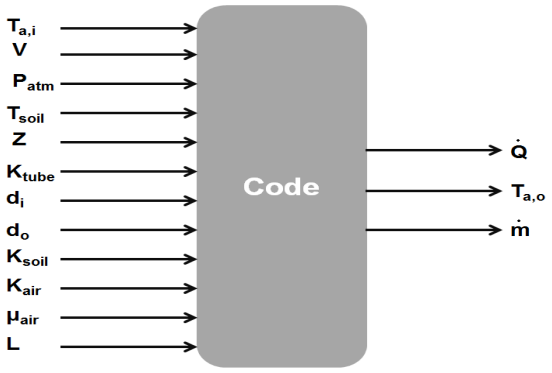

Fig. 3. Schematic of the inputs and outputs of the code

Based on the ambient air conditions (temperature, pressure, thermal conductivity, dynamic viscosity and specific heat), the characteristics of the buried tubes (inner and outer diameter, thermal conductivity and length), the characteristics of the soil (temperature, depth, and thermal conductivity) and speed of air within the tubes, a set of equations is solved in order to calculate the rate of heat loss by the air or the cooling capacity of the system, the outlet air temperature and the mass flow rate of the air flowing within the tubes.

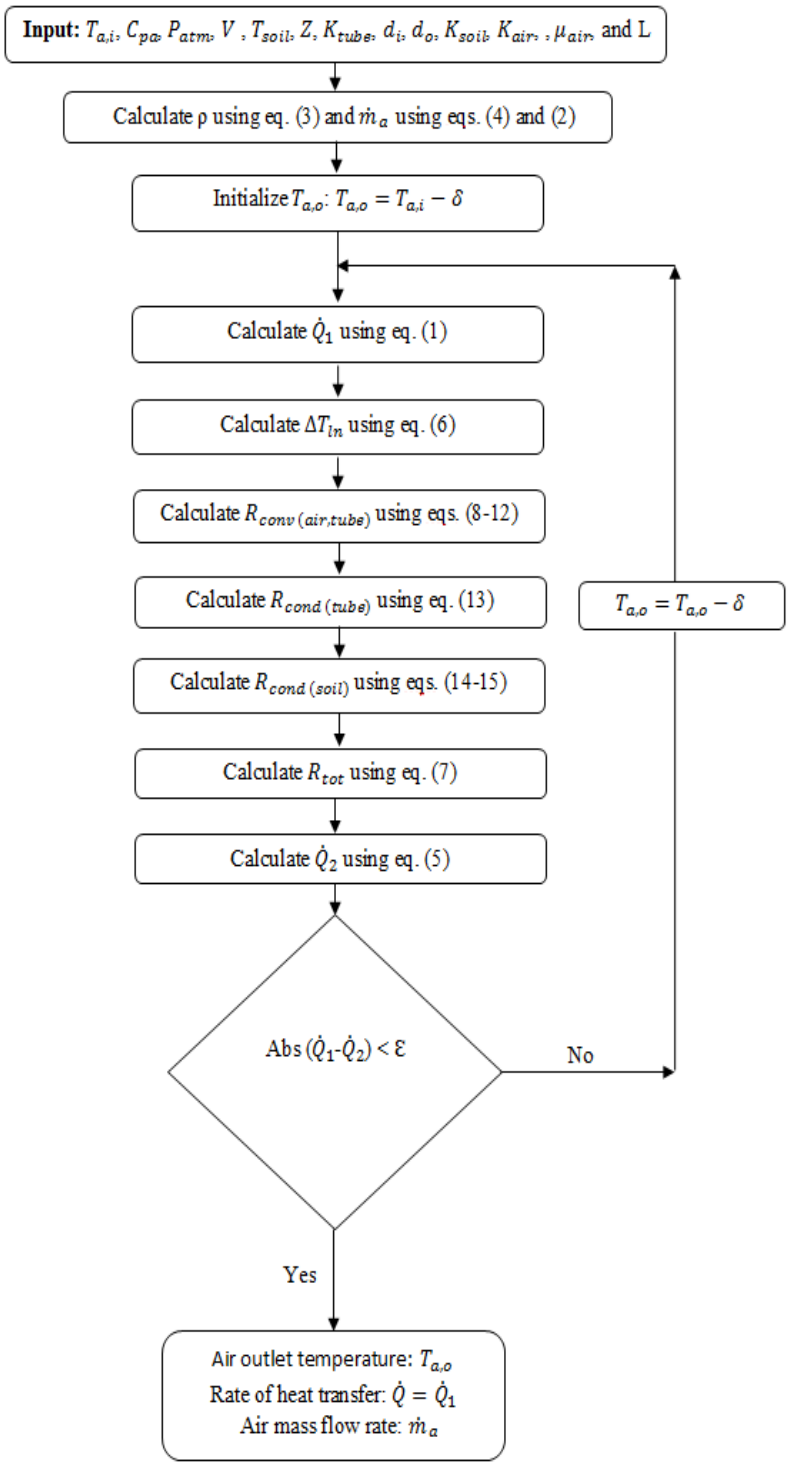

Fig. 4. Flow chart of the code developed

5- Experimental section

This section presents the experimental procedure (Section 5.1) to validate the thermal modelling and the developed computational code (Section 5.2).

5.1- Experimental procedure

Figure 5 shows a schematic of the experimental setup used in the experiments along with photos of the room (box) and buried pipes. A box of 1 m^3 that simulates a room and polyethylene tubes of 5.1 m length and 1.5 inches inner diameter are used. These tubes are buried in a box where 30 cm of soil could be placed around the tubes. Five k-type thermocouples with an uncertainty of ± 1% (on a Celcius Basis) are used to measure the temperature at the inlet and outlet of the tubes, inside the box (room), at the outlet of the box and the temperature of the soil. An anemometer with an uncertainty of ± 2% is used to measure the velocity of air flowing through the tubes and a fan is placed with a control valve to regulate the speed of air within the tubes. Fig. 5-a shows a schematic of the prototype with all used devices and Fig. 5-b and Fig. 5-c show photos of the prototype of the air cooling system by using buried tubes.

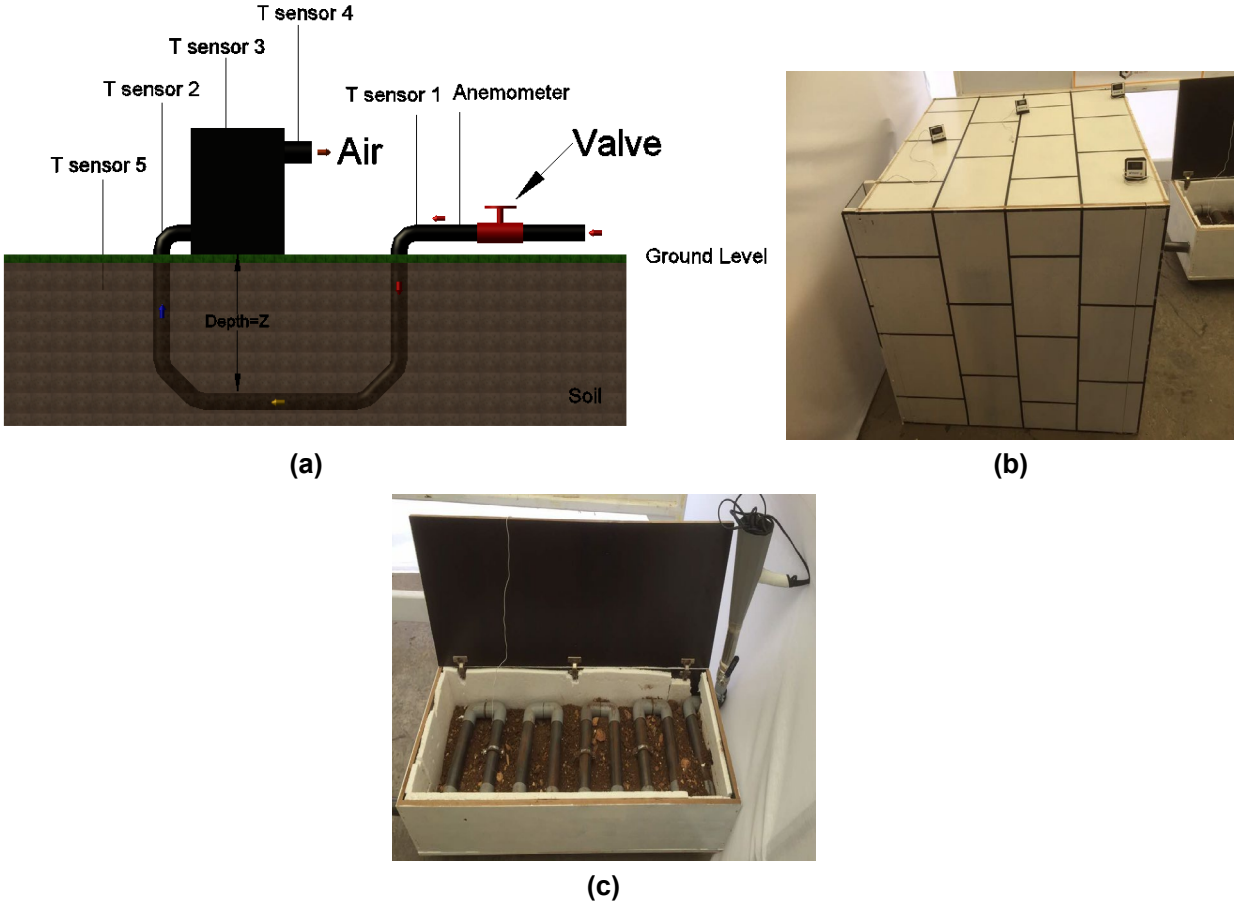

Figure 5: (a) Schematic of the whole prototype, (b) Photo of the box (room) with the four thermocouples, and (c) Photo of the box containing the buried tubes.

This prototype of the air cooling system by using buried tubes has been used for ambient conditions $T_{a,i}$ of around 30°C and atmospheric pressure of 101 kPa. The temperature of the soil is maintained around 10°C. Air speed and then air mass flow rate are controlled by the fan and the control valve.

5.2- Comparison Numerical-Experimental Data

Experiments have been done for different air speeds. Figure 6-a shows the results of the temperature of air at the outlet of the tubes in function of the air speed for the air cooling model and the experiments and Figure 6-b shows the relative error between numerical and experimental results.

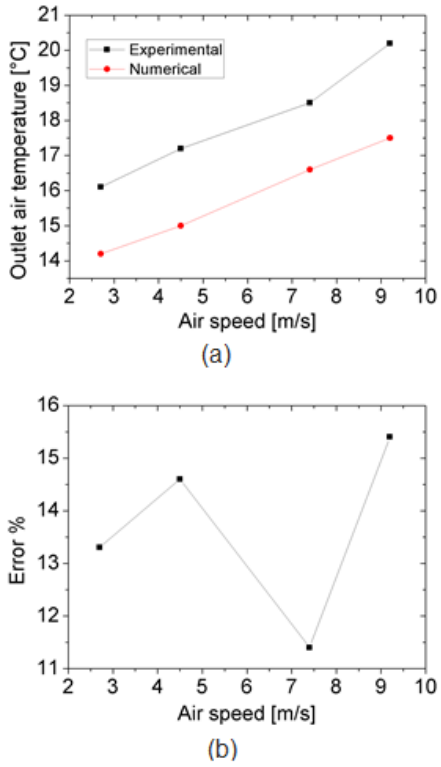

Fig. 6. (a) Air outlet temperature and (b) relative error of calculating air outlet temperature in function of air speed.

As shown in Figure 6-a, when the air speed and then the air mass flow rate through the tubes increases, the air outlet temperature increases for both, the model and the experiment since, for a same heat transfer rate, increasing the mass flow rate leads to an increasing in the outlet temperature. Furthermore, Figure 6-b shows that the relative error on the air outlet temperature between the model and the experiment is consistently below 16%. As illustration, for an air speed of 2.7 m/s, the air outlet temperatures of the model and the experiment are 14.2°C and 16.1°C respectively. The error on the air outlet temperature is then around 13.3%. For an air speed of 9.2 m/s, the air outlet temperatures of the model and the experiment are 17.5°C and 20.2°C respectively and the error is 15.4%.

Based on the above comparative results, the thermal modeling and the in-house computational code can be considered accurate and can be used to perform parametric and case studies.

6- Parametric study

A parametric study is performed to evaluate the performance of the proposed system in function of different key-parameters like: the air flow rate, the tubes length, the depth in soil and the tubes inner diameter.

6.1- Effect of the air flow

The computational code is used to evaluate the impact of the air flow rate on the thermal capacity of the tubes and the air outlet temperature which represent the thermal performance for three different depths. Fig. 7-a and Fig. 7-b show these results for an air inlet temperature of 30°C, a soil temperature of 10°C, a tubes length of 32 m and a tubes inner diameter of 20 cm.

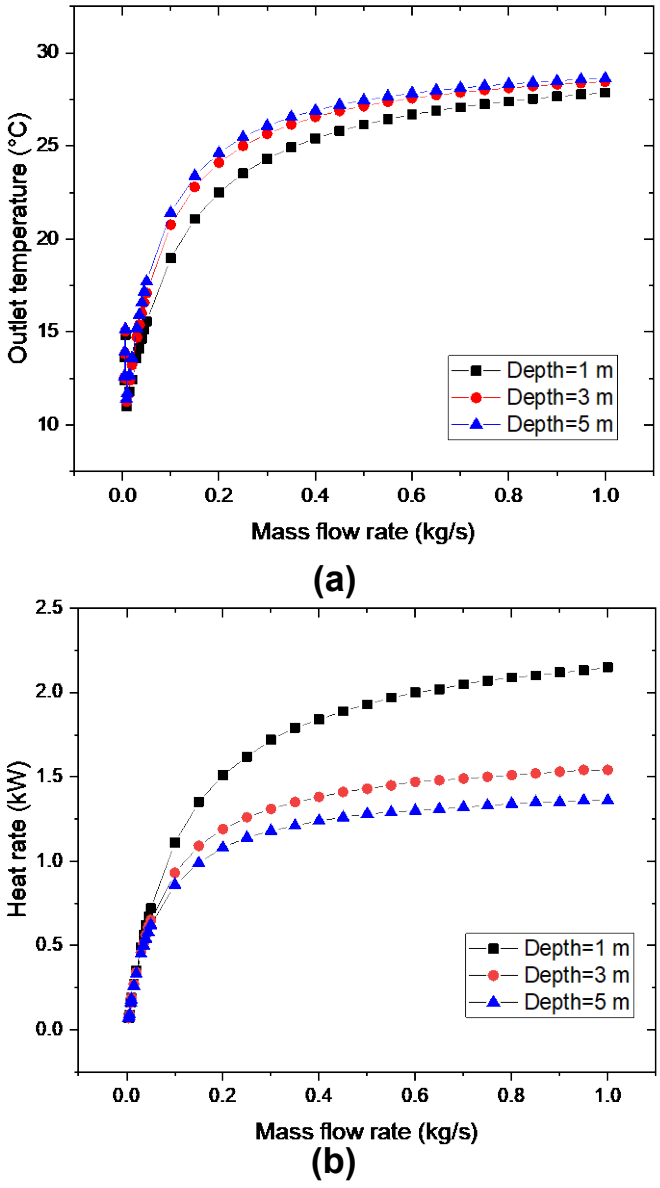

Fig. 7. Simulations results for (a) air outlet temperature and (b) heat rate in function of air flow rate for different depths.

Figure 7-a shows that a fluctuation in the air outlet temperature occurs at low air flow rate between 0.006 kg/s and 0.008 kg/s due to the transition from laminar flow to turbulent flow (Reynolds Number varying from 2111 to 2815) then it increases for the three different depths. But, the outlet temperature becomes almost invariable starting a given air flow rate for each depth.

As illustration, the outlet temperature becomes invariable at 26.7°C, 28.1 °C and 28.3 °C when the flow rate reaches 0.6 kg/s, 0.75 kg/s and 0.8 kg/s for soil depth of 1 m, 3 m, and 5 m respectively. The main reason behind is the heat transfer that becomes limited between the air stream and soil.

Moreover, Fig. 7-b shows that the thermal capacity of the tubes (heat lost by the air) increases when the air flow rate increases for the three depths. But for each depth, Fig. 7-b also shows that this thermal capacity increases suddenly between flow rates 0.006 kg/s and 0.008 kg/s due to the transition from laminar to turbulent flow. This will increase heat transfer coefficient (convective). Also, the thermal capacity becomes almost invariable starting a given air flow rate for each depth.

As illustration, the heat rate becomes invariable at 2 kW, 1.5 kW and 1.35 kW when the flow rate reaches 0.6 kg/s, 0.75 kg/s and 0.8 kg/s for depth of 1 m, 3 m, and 5 m respectively. The main reason behind is the heat transfer that becomes limited between the air stream and soil.

To quantify the results and shed lights on the importance of the new suggested concept, if one small apartment with a flow rate of 0.005 kg/s is considered, the buried pipe outlet temperature is 13.65 °C and the heat rate is 0.08 kW for a depth of 1 m. However, if four apartments with a total flow rate of 0.02 kg/s are considered, the buried pipe outlet temperature and heat rate become 12.44 °C and 0.35 kW respectively for same depth. This means that when the flow rate is increased 4 times the heat rate obtained with the new system increased 4.38 times instead of 4 times if one single heat exchanger is used for each apartment. This underline the main advantage of the suggested concept.

Now, if a house with a flow rate of 0.45 kg/s is taken under study, the buried pipe outlet temperature is 24.3°C and the heat rate is 1.72 kW for a depth of 1 m. However, if two houses with a total flow rate of 0.9 kg/s are considered, the buried pipe outlet temperature and heat rate become 27.7°C and 2.12 kW respectively for same depth. The gain in heat rate between these 2 cases is not as high as in the first case study since the flow is turbulent in both cases and there is a limitation in heat transfer for high flow rates.

Two main recommendations can be raised based on the features mentioned above:

1. When the flow rate is high (highly turbulent), it is recommended to use more than one buried tube exchanger for all residences.
2. When the flow rate coming from each residence is low (laminar or slightly turbulent), it is beneficial to use one buried tube exchanger for all residences.

6.2- Effect of the tubes length and depth in soil

The in-house code software is now used to study the impact of the tubes length "L" on the heat rate and the temperature of the air leaving the buried tubes and entering the room. Fig. 8 shows these results for an air inlet temperature of 30°C, a soil temperature of 10°C, an air speed of 4 m/s, tubes inner diameter of 20 cm and for different depths. This air speed corresponds then to an air mass flow rate of 0.145 kg/s.

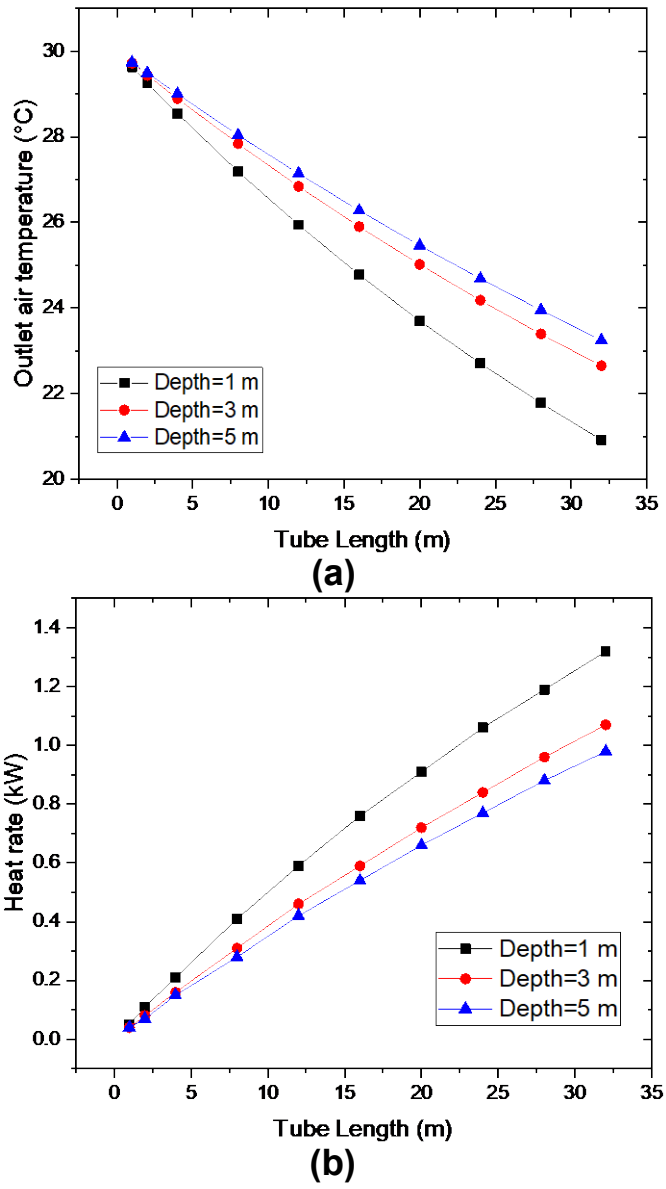

Fig. 8. Simulations results for (a) air outlet temperature and (b) heat rate in function of tubes length for three different depths in soil.

Fig. 8-a and Fig. 8-b show that the air outlet temperature decreases and the heat rate increases when the tubes length increases for the three depths. When the tubes length increases, the heat exchange surface between the soil and the air flowing inside the tubes (which is the lateral area of the tubes) increases. The rate of heat transfer is then increased. When the depth in soil increases, the air outlet temperature increases (for same tube length) because the conductive resistance of the soil increases with the depth. This leads to a decrease in the rate of heat exchange and thus to an increase in the outlet air temperature.

As illustration, for a depth of 1 m and for a tube length of 1 m, the outlet temperature is 29.6°C. When this length is equal to 32 m, the outlet temperature decreases to 20.9°C. For a depth of 5 m and for a tube length of 1 m, the outlet temperature is 29.8°C; it decreases to 23.3°C when the length is equal to 32 m.

6.3- Effect of the buried tubes diameter

The in-house code software is now used to study the impact of the tubes inner diameter "d_i" on the heat rate and the temperature of the air leaving the buried tubes and entering the room. Fig. 9 shows these results for an air inlet temperature of 30°C, a soil temperature of 10°C, a soil depth of 2 m, an air mass flow rate of 0.145 kg/s and different tubes lengths.

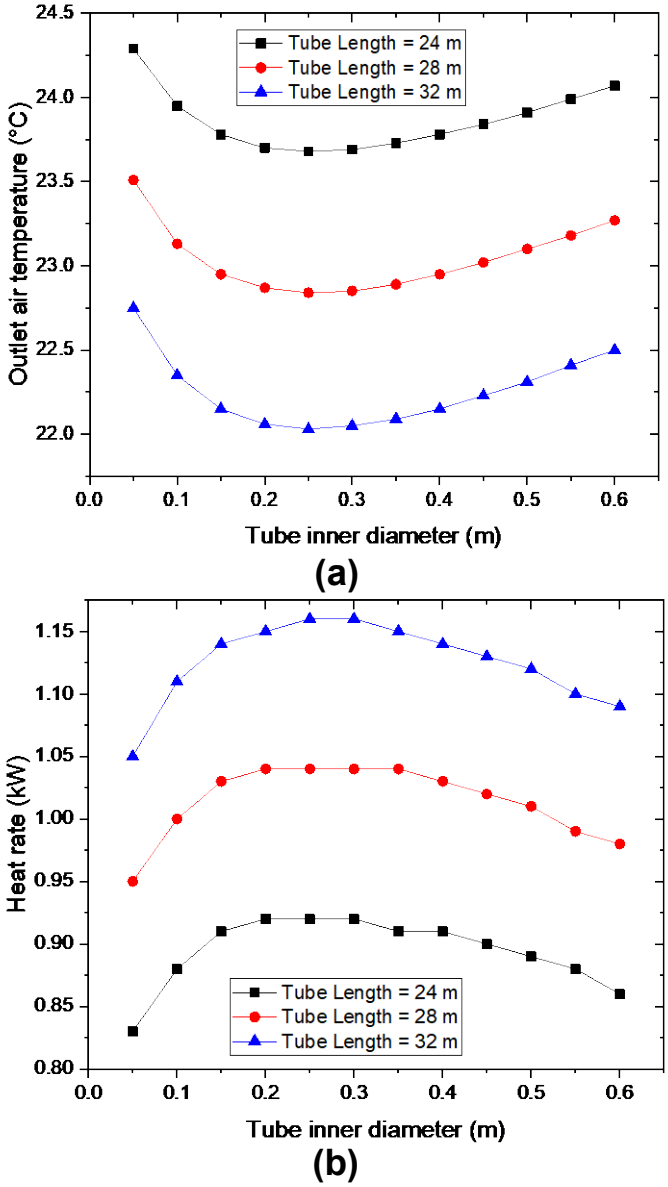

Fig. 9. Simulations results for (a) air outlet temperature and (b) heat rate in function of tubes inner diameter and length.

Fig. 9-a and Fig. 9-b show that the air outlet temperature has a minimum and the heat rate has a maximum in function of the tube diameter for the three lengths. As illustration, the minimum air outlet temperature is 23.7 °C and the maximum heat rate is 0.92 kW for tube inner diameter of 0.25 m and length of 24 m. The minimum air outlet temperature and the maximum heat rate become 22.03 °C and 1.16 kW respectively for tube inner diameter of 0.25 m and length of 32 m.

This trend is mainly due to the convective thermal resistance of the air inside the tubes and the conductive thermal resistance of the soil that depend on the tubes diameter. Fig. 10 shows the variation of these thermal resistances in function of the tubes inner diameter "d_i" for same conditions and for a tube length of 32 m.

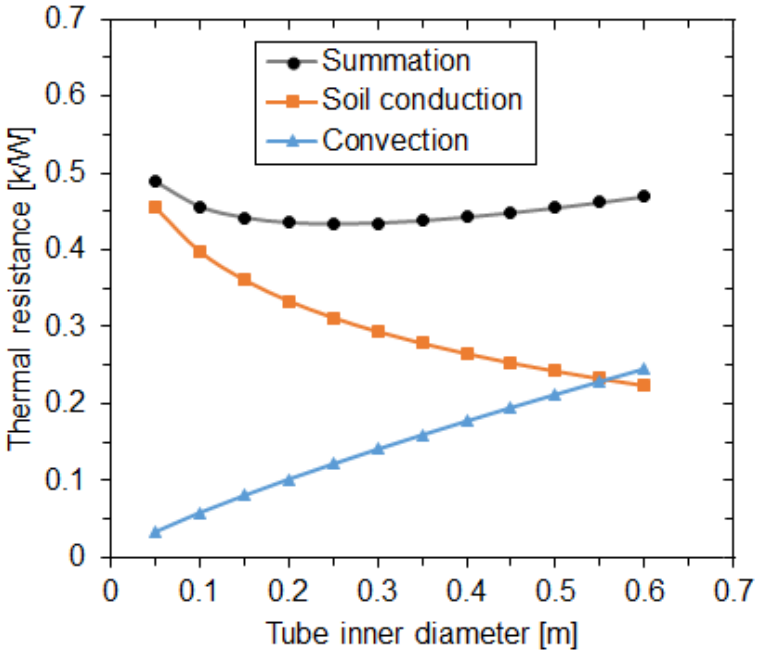

Fig. 10. Simulations results for thermal resistances in function of tubes inner diameter.

Fig. 10 shows that the convective thermal resistance of the air inside the tubes increases when the tubes inner diameter increases. When the inner diameter increases, the air speed and then the Reynolds number decrease which leads to a decrease of the convective heat transfer coefficient between the air and the inner surface of the tubes and then to an increase of the convective thermal resistance. Also, Fig.10 shows that the conductive thermal resistance of the soil decreases when the tubes inner diameter increases since this resistance is calculated by using eqs. (14) and (15). The summation of these two resistances is also shown in Fig.10. This summation has a minimum for an inner diameter of 0.25 m.

7- Case study

The performance of the proposed cooling system is evaluated in this section. The objective is to evaluate the amount of electrical energy that can be decreased per month when a residence is completely cooled or pre-cooled by the geothermal air cooling system. Then, the amount of the electric energy saved is calculated and the monthly amount of CO_2 emissions reduction is evaluated.

For that purpose, an electrical vapor compression refrigeration cooling system of 3.52 kW (12000 Btu/hr = 1 ton) cooling capacity is taken under study where it is turned on for 240 hours/month when the outer temperature is 30°C and a relative humidity of 80%. This case has been designed in order to simulate a typical residence requirements located in Beirut City. The energy reduced per month by utilizing the geothermal cooling system instead of the geothermal cooling system can be calculated using equations (16) and (17).

$$E_{reduced\,/\,month} = \frac{\dot{Q}_{Geothermal}}{\beta} \cdot t_r \qquad (16)$$

Where:

- $E_{reduced/month}$ is the monthly energy reduced, kWh/month;
- $\dot{Q}_{Geothermal}$ is the cooling capacity ensured by the geothermal system (calculated by using equation (1), kW;
- t_r is the running time of the system (assumed to be 8 hrs./day and 30 days/month), hrs./month;
- β is the coefficient of performance of the refrigeration cooling system. This coefficient is defined as the ratio of the cooling capacity of this system and the electric power consumed by it.

Fig. 11 shows the results of the amount of energy reduced as function of the tubes length and for different coefficients of performance for an air inlet temperature of 30°C, a soil temperature of 10°C, a soil depth of 2 m, an air speed and mass flow rate of 4 m/s and 0.145 kg/s respectively and tubes inner diameter of 20 cm.

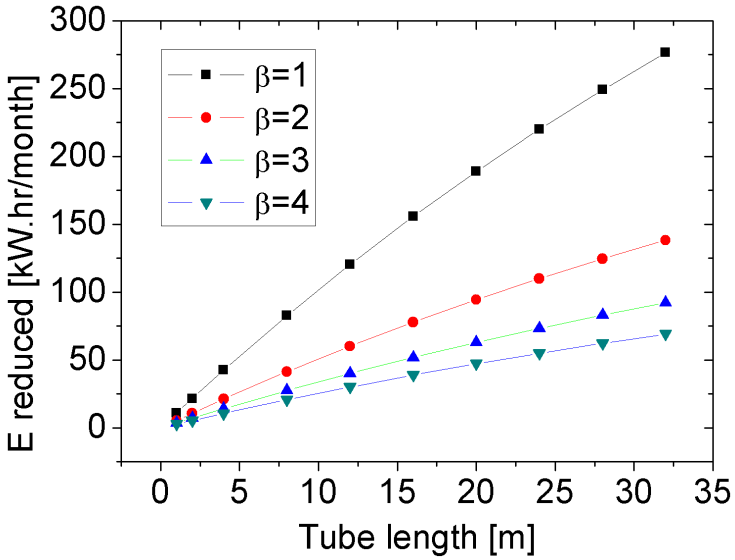

Fig. 11. Variation of the energy reduced as function of tubes length for different coefficients of performance.

As shown in Fig. 11, the amount of energy reduction increases when the tubes length increases for the four coefficients of performance since the air is cooled more when passing through the buried tubes because the lateral area which is the heat exchange area increases which leads to the increase of the cooling capacity ensured by the geothermal system. Also, Fig. 11 shows that the amount of energy reduction is more important when the coefficient of performance is low. As illustration, for a tubes length of 1 m, the amount of energy reduction is 11 kWh, 5.52 kWh, 3.68 kWh and 2.76 kWh for a coefficient of performance of 1, 2, 3 and 4 respectively. This amount of energy reduction becomes 276.5 kWh, 138.2 kWh, 92.2 kWh and 69.1 kWh for a coefficient of performance of 1, 2, 3 and 4 respectively for a tubes length of 32 m.

Reducing the electric energy consumed by using the geothermal cooling systems causes a decrease in the CO_2 emissions to the atmosphere which is calculated by using the following equation:

$$M_{reduced,CO_2} = E_{reduced/month} \cdot M_{CO_2/1kWh} \quad (18)$$

Where:

- $M_{reduced,CO_2}$ is the amount of CO_2 emission reduced, kg;

– $M_{CO_2/1kWh}$ is the amount of CO_2 emitted after producing 1 kWh of electricity. This value is approximately equal to 0.71 in Lebanon. It can be noted that the electricity in Lebanon is mainly generated by systems that use conventional sources.

Fig. 12 shows the variation of the amount of CO_2 emission reduction in one month in terms of the tubes length and for different coefficients of performance.

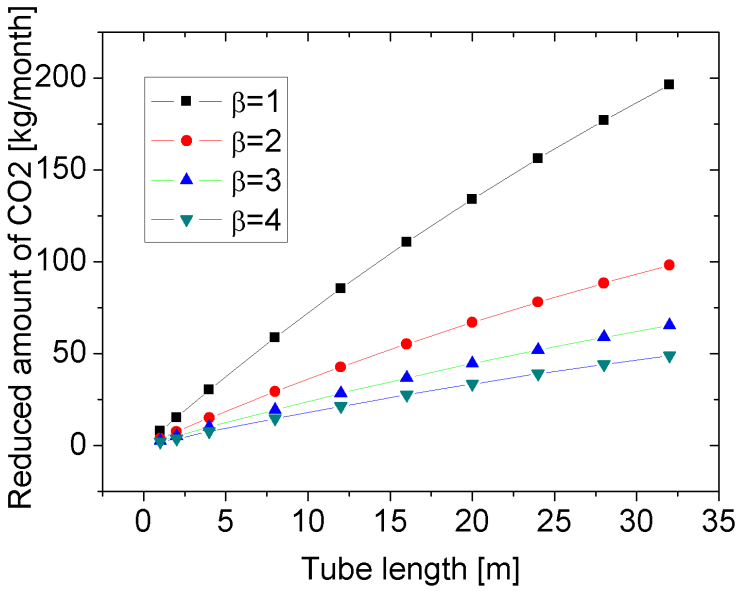

Fig. 12. Variation of amount of reduced CO_2 emission as function of tubes length for different coefficients of performance.

As shown in Fig. 12, the amount of CO_2 emissions reduction increases when the tubes length increases for the four coefficients of performance. Also, Fig. 12 shows that this amount is much more important when the coefficient of performance is low. In order of magnitudes, the amount of CO_2 emissions reduction increases from 7.8 kg to 196.3 kg, 3.9 kg to 98.2 kg, 2.6 kg to 65.4 kg and from 1.96 kg to 49.1 kg for the coefficients of performance 1, 2, 3 and 4 respectively, as the tubes length increases from 1 m to 32 m.

8- Conclusions

The present manuscript concerned a complete numerical and experimental study of the performance of a cooling system that uses buried pipes as geothermal energy. A thermal, energetic and environmental modelling of the system is carried out and experiments are conducted to validate the numerical results. The main results of the work are summarized below:

1. The model predicts well the outlet temperature of the air with an error between varying between 11 and 16 % between numerical and experimental results for different air speeds.
2. When the flow rate is high (highly turbulent), it is recommended to use more than one buried tube exchanger for all residences.
3. When the flow rate coming from each residence is low (laminar or slightly turbulent), it is beneficial to use one buried tube exchanger for all residences.

4. When the tubes length increases, the air outlet temperature decreases and when the depth increases, the air outlet temperature increases. For instance, when the tube length increases from 1 to 32 m, the temperature decreases from 29.6°C to 20.9°C (for a depth of 1 m) and when the depth in soil increases from 1 m to 5 m, the outlet air temperature increases from 20.9°C to 23.3°C (for a pipe length of 32 m).
5. The air outlet temperature has a minimum for an inner diameter of 0.25 m. The convective thermal resistance of air increases when the tubes inner diameter increases because the air speed and Reynolds number decreases but the soil conductive thermal resistance decreases. Their summation has a minimum at 0.25 m.
6. When the tube length increases from 1 m to 32 m, the amount of reduced energy increases from 3.68 kWh to 138.2 kWh, and the amount of CO_2 emissions reduction increases from 3.9 kg to 98.2 kg per month in comparison with a conventional refrigeration cooling system having a coefficient of performance of 2.

References

[1] M. Nadarajan and V. Kirubakaran, "Simulation studies on small rural residential houses using sustainable building materials for thermal comfort – case comparison", Advances in Building Energy Research, Vol 11, pp 193-207, 2017. https://doi.org/10.1080/17512549.2016.1215260.

[2] P. Fazil Hassan, K. Jothi Prakash and V. Kirubakaran, "Experimental investigation of energy efficient building for passive heating/cooling", International Journal of Energy Technology and Policy, Vol. 11, pp 246-253, 2015.

[3] E. Amores, M. Sánchez-Molina, and M. Sánchez, Effects of the marine atmosphere on the components of an alkaline water electrolysis cell for hydrogen production, Results in Engineering, 10 (2021) 100235. https://doi.org/10.1016/j.rineng.2021.100235.

[4] F. B. Elehinafe, O. A. Odunlami, A. O. Mamudu, and O. O. Akinsanya, Investigation of the potentials of southwest Nigerian Napier Grass as an energy source to replace fossils used in firing thermal power plants for air emissions control, Results in Engineering, 11 (2021) 100259. https://doi.org/10.1016/j.rineng.2021.100259.

[5] U. K. Elinwa, J. E. Ogbeba, and O. P. Agboola, Cleaner energy in Nigeria residential housing, Results in Engineering, 9 (2021) 100103. https://doi.org/10.1016/j.rineng.2020.100103.

[6] Ahmad Jahanbakhshi, Somayeh Karami-Boozhani, Mojtaba Yousefi, Jong Boon Ooi, Performance of bioethanol and diesel fuel by thermodynamic simulation of the miller cycle in the diesel engine, Results in Engineering, 12 (2021) 100279. https://doi.org/10.1016/j.rineng.2021.100279.

[7] G. Fabbri and M. Greppi, Numerical modeling of a new integrated PV-TE cooling system and support, Results in Engineering, 11 (2021) 100240. https://doi.org/10.1016/j.rineng.2021.100240.

[8] N. Raj, S. Arputham and V. Kirubakaran, "Simulation and experimental study on performance analysis of solar photovoltaic integrated thermoelectric cooler using MATLAB Simulink", Thermal Science, pp 301, 2021. https://doi.org/10.2298/TSCI201211301N.

[9] S. Arputham, N. Raj and V. Kirubakaran, "Monitoring and simulation of parabolic trough collector powered vapor absorption refrigeration system for rural cold storage", Thermal Science, pp 298, 2021. https://doi.org/10.2298/TSCI201110298S.

[10] P. R. G. N. Lalith, G. Prabakaran, A. Murugaiyan and V. Kirubakaran, "Hybrid Photovoltaic-Thermal Systems: Innovative CHP approach," 4th International Conference on Electrical Energy Systems (ICEES), pp. 726-730, 2018. doi: 10.1109/ICEES.2018.8442352.

[11] Susan Susan, Dyah Wardhani, Building integrated photovoltaic as GREENSHIP'S on site renewable energy tool, Results in Engineering, 7 (2020) 100153. https://doi.org/10.1016/j.rineng.2020.100153.

[12] J. Thakur, S. Rauner, N. Darghouth and B. Chakraborty, "Exploring the impact of increased solar deployment levels on residential electricity bills in India", Renewable energy, Vol 120, pp 512-523, 2018. https://doi.org/10.1016/j.renene.2017.12.101.

[13] K. Balasubramanian, S. Thanikanti, U. Subramaniam, N. Sudhakar and S. Sichilalu, " A novel review on optimization techniques used in wind farm modelling", Renewable Energy Focus, Vol 35, 2020. https://doi.org/10.1016/j.ref.2020.09.001.

[14] C. Martinez-Anido, G. Brinkman, B. Hodge, "The impact of wind power on electricity prices", Renewable Energy, Vol 94, pp 474-487, 2016. https://doi.org/10.1016/j.renene.2016.03.053.

[15] L. Zeng, G. Li, M. Li, Z. Feng, L. Yang and X. Luo, " Design and experimental performance of an off-grid ice storage system driven by distributed wind energy ", Energy & Buildings, Vol 224, 110252, 2020. https://doi.org/10.1016/j.enbuild.2020.110252.

[16] A. Fragaki, T. Markvart, and G. Laskos, "All UK electricity supplied by wind and photovoltaics – The 30–30 rule", Energy, Vol 169, pp. 228-237, 2019. https://doi.org/10.1016/j.energy.2018.11.151.

[17] W. Stanek, B. Mendecka, L. Lombardi, T. Simla, "Environmental assessment of wind turbine systems based on thermo-ecological cost", Energy, Vol 160, pp. 341-348, 2018. https://doi.org/10.1016/j.energy.2018.07.03.

[18] G. Ren, J. Wan, J. Liu, D. Yu, L. Söder, " Analysis of wind power intermittency based on historical wind power data", Energy, Vol 150, pp. 482-492, 2018. https://doi.org/10.1016/j.energy.2018.02.142.

[19] A. Ferrantelli, J. Fadejev and J. Kurnitski, "A tabulated sizing method for the early stage design of geothermal energy piles including thermal storage", Energy & Buildings, Vol 223, 110178, 2020. https://doi.org/10.1016/j.enbuild.2020.110178.

[20] F. Calise, S. Di Fraia, A. Macaluso, N. Massarotti and L.Vanoli, " A geothermal energy system for wastewater sludge drying and electricity production in a small island", Energy, Vol 163, pp 130-143, 2018. https://doi.org/10.1016/j.enbuild.2020.110178.

[21] L. Ozgenera, A. Hepbaslib and I. Dincer, "Energy and exergy analysis of geothermal district heating systems: an application", Building and Environment, Vol 40, pp 1309-1322, 2005. https://doi.org/10.1016/j.buildenv.2004.11.001.

[22] D. Moya, C. Aldás and P. Kaparaju, "Geothermal energy: Power plant technology and direct heat applications", Renewable and Sustainable Energy Reviews, Vol 94, pp 889-901, 2018. https://doi.org/10.1016/j.rser.2018.06.047.

[23] K. Kavadias, P. Alexopoulos, G. Charis and J. Kaldellis, "Sizing of a solar–geothermal hybrid power plant in remote island electrical network", Energy Procedia, Vol 157, pp 901-908, 2018. https://doi.org/10.1016/j.egypro.2018.11.256

[24] S. Van Erdeweghe, J. Van Bael, B. Laenen and W. D'haeseleer, "Design and off-design optimization procedure for low-temperature geothermal organic Rankine cycles", Applied Energy, Vol 242, pp 716-731, 2019. https://doi.org/10.1016/j.apenergy.2019.03.142.

[25] E. Akrami, A. Chitsaz, H. Nami, and S. Mahmoudi, "Energetic and exergo-economic assessment of a multi-generation energy system based on indirect use of geothermal energy", Energy, Vol 124, pp 625-639, 2017. https://doi.org/10.1016/j.energy.2017.02.006.

[26] M. Kaushal, "Performance analysis of clean energy using geothermal earth to air heat exchanger (GEAHE) in Lower Himalayan Region – Case study scenario", Energy & Buildings, Vol 248, 111166, 2021. https://doi.org/10.1016/J.ENBUILD.2021.111166.

[27] M. Santamouris, G. Mihalakakou, C. Balaras, A. Argiriou, D. Asimakopoulos and M. Vallindras, "Use of buried pipes for energy conservation in cooling of agricultural greenhouses", Solar Energy, Vol 55, pp 111-124, 1995. https://doi.org/10.1016/0038-092X(95)00028-P.

[28] S. Ahmed, M. Amanullah, M. Khan, M. Rasul and N. Hassan, "Parametric study on thermal performance of horizontal earth pipe cooling system in summer", Energy Conversion and Management, Vol 114, pp 324-337, 2016. https://doi.org/10.1016/j.enconman.2016.01.061.

[29] P. Hollmuller and B. Lachal, “Cooling and preheating with buried pipe systems: monitoring, simulation and economic aspects”, Energy and Buildings, Vol 33, pp 509-518, 2001. https://doi.org/10.1016/S0378-7788(00)00105-5.

[30] D. Yang and J. Zhang, “Analysis and experiments on the periodically fluctuating air temperature in a building with earth-air tube ventilation”, Building and Environment, Vol 85, pp 29-39, 2015. https://doi.org/10.1016/j.buildenv.2014.11.019.

[31] V. Bansal, R. Misra, G. Agrawal and J, Mathur, “Performance analysis of earth–pipe–air heat exchanger for summer cooling”, Energy and Buildings, Vol 42, pp 645-648, 2010. https://doi.org/10.1016/j.enbuild.2009.11.001.

[32] M.Maerefat and A.P.Haghighi, “Passive cooling of buildings by using integrated earth to air heat exchanger and solar chimney”, Renewable Energy, Vol 35, pp 2316-2324, 2010. https://doi.org/10.1016/j.renene.2010.03.003.

[33] H. Li, Y. Yu, F. Niu, M. Shafik and B. Chen, “Performance of a coupled cooling system with earth-to-air heat exchanger and solar chimney”, Renewable Energy, Vol 62, pp 468-477, 2014. https://doi.org/10.1016/j.renene.2013.08.008.

[34] M. Bojic, N. Trifunovic, G. Papadakis, S. Kyritsis, “Numerical simulation, technical and economic evaluation of air-to-earth heat exchanger coupled to a building”, Energy, Vol 22, pp 1151-1158, 1997. https://doi.org/10.1016/S0360-5442(97)00055-8

[35] H. Wei, D. Yang, Y. Guo and M. Chen, “Coupling of earth-to-air heat exchangers and buoyancy for energy-efficient ventilation of buildings considering dynamic thermal behavior and cooling/heating capacity”, Energy, Vol 147, pp 587-602, 2018. https://doi.org/10.1016/j.energy.2018.01.067.

[36] A. Alsagri, A. Chiasson and M. Shahzad, “Geothermal Energy Technologies for Cooling and Refrigeration Systems: An Overview”, Arabian Journal for Science and Engineering, 2021. https://doi.org/10.1007/s13369-021-06296-x.

[37] I. Gondal, “Prospects of shallow geothermal systems in HVAC for NZEB”, Energy and Built Environment,Vol 2, pp 425-435, 2021. https://doi.org/10.1016/j.enbenv.2020.09.007.

[38] P. Ding, K. Zhang, Z. Yuan, Z. Wang, D. Li, T. Chen, J. Shang, and R. Shofahaei, “Multi-objective optimization and exergoeconomic analysis of geothermal-based electricity and cooling system using zeotropic mixtures as the working fluid”, Journal of Cleaner Production, Vol. 294, 2021. https://doi.org/10.1016/j.jclepro.2021.126237.

[39] M. Krarti and J.F. Kreider, “Analytical model for heat transfer in an underground air tunnel”, Energy Conversion and Management, Vol 37, pp. 1561-1574, 1996. https://doi.org/10.1016/0196-8904(95)00208-1.

[40] F. Al-Ajmi, D.L. Loveday and V.I. Hanby, “The cooling potential of earth–air heat exchangers for domestic buildings in a desert climate”, Building and Environment, Vol 41, pp. 235-244, 2006. https://doi.org/10.1016/j.buildenv.2005.01.027.

[41] R. Kumar, S.C. Kaushik and S.N. Garg, “Heating and cooling potential of an earth-to-air heat exchanger using artificial neural network”, Renewable Energy, Vol 31, pp. 1139-1155, 2006. https://doi.org/10.1016/j.renene.2005.06.007

[42] A. Shor, M. Khan and G. Ahteshamul-Haque, “Construction and Performance Study of an Underground Air Heating and Cooling System”, International Journal of Sustainable and Green Energy, Vol 5, pp 27-39, 2016. https://doi.org/10.11648/j.ijrse.20160503.11

[43] G. Mihalakakou, J. Lewis and M. Santamouris, “On the heating potential of buried pipes techniques application in Ireland”, Energy and Buildings, Vol. 24, pp. 19-25, 1996. https://doi.org/10.1016/0378-7788(95)00957-4.

[44] M. Dubey, J.L. Bhagoria, and A. lanjewar, “Earth Air Heat Exchanger in Parallel Connection”, International Journal of Engineering Trends and Technology, Vol 4, pp. 2463-2467, 2013.